PARAMETERS OF CASCADE GAMMA DECAY OF ^{153}Sm COMPOUND-STATES

Nguyen Ngoc Anh[1], *Nguyen Xuan Hai*[1], *Pham Dinh Khang*[1], *Ho Huu Thang*[1], *A.M. Sukhovoj*[2], *L.V. Mitsyna*[2]

[1]Vietnam Atomic Energy Institute,
[2]Joint Institute for Nuclear Research, Russia

Abstract

From the researches of gamma-cascade intensities of 40 nuclei in the range of nuclear masses $40 \leq A \leq 200$ the conclusion was obtained that level density and radiation strength function of nuclei depend on a number of pair-breaking neutrons. A new practical model, which reproduces the experimental intensity of cascade data with a high accuracy, was also developed. This work presents a distribution of cascade gamma decay intensity of ^{153}Sm compound-states as a function of the primary gamma-transition energy. Obtained results confirm the previous available data.

Introduction

Up to now, the study of intensities of two-step gamma-cascades at compound nuclei decaying is the efficient experimental method to study the properties of highly excited states below the binding energy B_n.

Radiation strength functions $k = \Gamma_{\lambda i}/(E_\gamma^3 \times A^{\frac{2}{3}} \times D_\gamma)$ and a level density ρ of nucleus determine the total radiation width Γ_γ and cascade intensity $I_{\gamma\gamma}$ in compound nucleus [1] as:

$$\Gamma_\gamma = \langle \Gamma_{\lambda i} \rangle \times m_{\lambda i} \qquad (1)$$

$$I_{\gamma\gamma} = \sum_{\lambda,f} \sum_i \frac{\Gamma_{\lambda i}}{\Gamma_\lambda} \frac{\Gamma_{if}}{\Gamma_i} = \sum_{\lambda,f} \frac{\Gamma_{\lambda i}}{\langle \Gamma_{\lambda i} \rangle m_{\lambda i}} n_{\lambda i} \frac{\Gamma_{if}}{\langle \Gamma_{if} \rangle m_{if}} \qquad (2)$$

Here

$\Gamma_{\lambda i}$ is the partial width of primary γ-transition from an excited level λ to an intermediate level i,

Γ_{if} is the partial width of secondary γ-transition to the lower level f,

$m_{\lambda i}$ is a number of initial excited primary transitions in energy interval from E_λ to E_i,

m_{if} is a number of initial excited secondary γ-transitions in energy interval from E_i to E_f,

$n_{\lambda i}$ is a number of intermediate levels of cascade in small intervals of the energies of initial transitions,

and D_γ is the spacing between nuclear levels.

The study of cascade intensities of 40 nuclei in the range of nuclear mass $40 \leq A \leq 200$ deduced that the density ρ of excited levels and radiation strength functions k are determined by a number of excited quasi-particles and by a number of phonon excitations [2, 3] at any energy of level i.

A new practical model for determination of level densities and strength functions was developed using a system of equations (2) was developed [4].

This work studies parameters of cascade intensities of ^{153}Sm in thermal neutron capture reaction.

Experiment

Experiment was performed with event-event gamma coincidence spectrometer, which is installed at the tangential beam port of Dalat Nuclear Research Reactor (DNRR). The target sample was made from Samarium Oxide which has high enrichment isotope of ^{152}Sm [12], the sample was placed between two HPGe detectors (detector type of GMX35 with relative efficiencies are 35 and 38 % respectively) and set at 45^{o} from neutron beam. Experimental data were collected for an approximately 300 hours.

The thermal neutron beam was filtered by sulfur, lead and silicon; the neutron flux is about 5×10^{5} n·cm^{-2}·s^{-1} at sample irradiation position. The cadmium ratio is about 900 (using 1 mm thickness of cadmium cover). The neutron beam was collimated by a mixture of paraffin and boron. The distance between the end capsule of detectors and neutron beam center was 5 cm. Two detectors were surrounded by lead of 10 cm thickness for shielding against gamma rays in the environment. The integral background count rate of the spectrometer in the $0.5 \div 8$ MeV gamma energy range was less than 400 counts per second. The transfer of gamma radiation between detectors, which includes Compton-backscattered and X-ray, was suppressed by two lead filter plates of 2 mm thickness placed between sample and detectors [3].

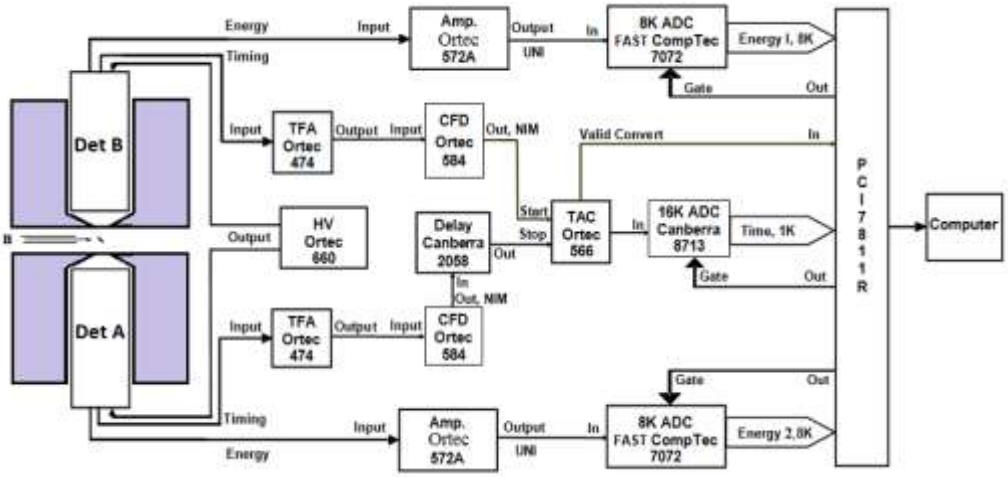

Fig.1. The electronics configuration.

The electronic configuration of coincidence spectrometer that was used in this experiment is shown in Fig. 1. The detector energy signals are amplified and shaped into Gaussian pulse by 572 amplifier (AMP) modules with a shaping time of 3 μs and energy gain of about 0.85 keV per channel. The output signals amplitude of 572 AMPswere converted to digital number by a 7072 dual analog-to-digital converter (ADC) module with selection of 8192 channels for a maximum 10V input pulse. The low-level discriminators of ADCs 7072 were set at 520 keV energy gamma rays. The timing signals are connected with 474 timing filter amplifier (TFA) modules for amplifying and filtering. The output signals of TFAs 474 were plugged into 584 constant fraction discriminator (CFD) modules, which were used in slow rise time rejection (SRT) mode. The CFD's output signal of the second channel (using Det B) was used for start signal for 566 time-to-amplitude converter (TAC). The CFD's output signal of first channel was delayed 35 nanosecond (ns) and used for TAC's stop signal.

TAC range was set at 100 ns. TAC output signal was digitized in 8713 ADC with selection of 512 channels for a maximum 10 V input pulse. ADC 7072 was gated by TAC's "Valid Convert" signal. The delay for synchronizing was 6 μs and set by interface software which was set up in event – event coincidence mode. The recorded data included coincidence gamma-rays energy from two detectors and time interval between two gamma rays of pair events.

The recorded data were analyzed off-line by Summing of Amplitude Coincident Pulses (SACP) method.

Analysis

Most of useful information of SACP method was given in sum coincidence spectrum. Main part of SACP spectra of ^{153}Sm is shown in Fig.2.

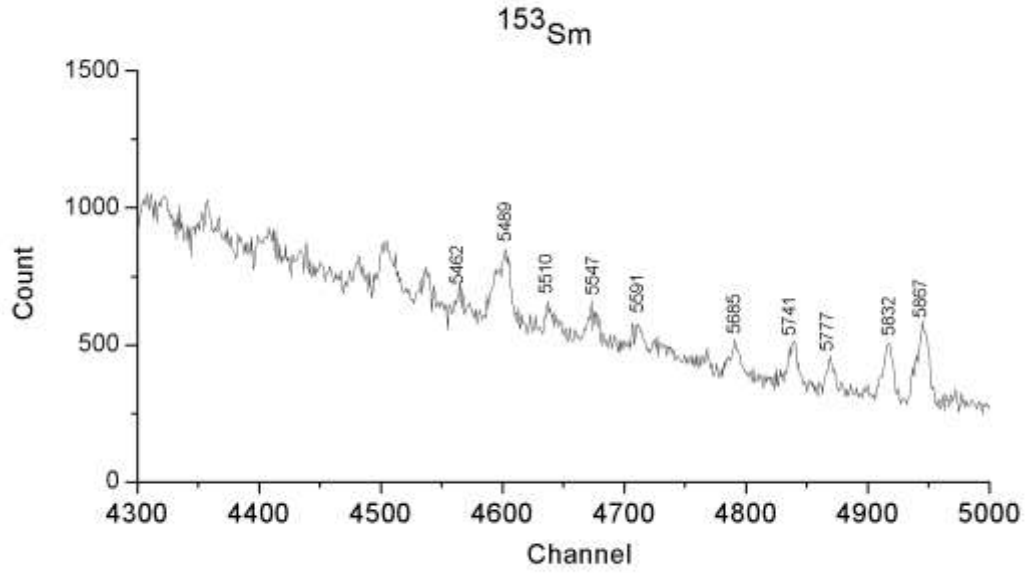

Fig. 2. Main part of the sum coincidence spectrum of ^{153}Sm. Full-energy peaks are labelled with the energy (in keV).

From each sum peak in sum coincidence spectrum, a two-step cascade spectrum (TSC) was obtained by choosing pairs of event with $E_{sum} - \Delta E \leq E_1 + E_2 \leq E_{sum} + \Delta E$. Fig. 3 shows a TSC in case $E_1 + E_2 = 5867.60$ keV.

The use of the method of improvement of the resolution without decrease in registration efficiency [6] improves TSC spectra resolution by 1.2-2.6 times. In TSC spectra, each two-step cascade is presented by a pair of peaks with equal area and widths [5]. The cascade decay events were determined by identifying appropriate peaks in TSC spectra. Their relative intensities were obtained from peaks area. The amount of experimental data allowed us to construct a level scheme of ^{153}Sm [7] and to calculate another nuclear properties.

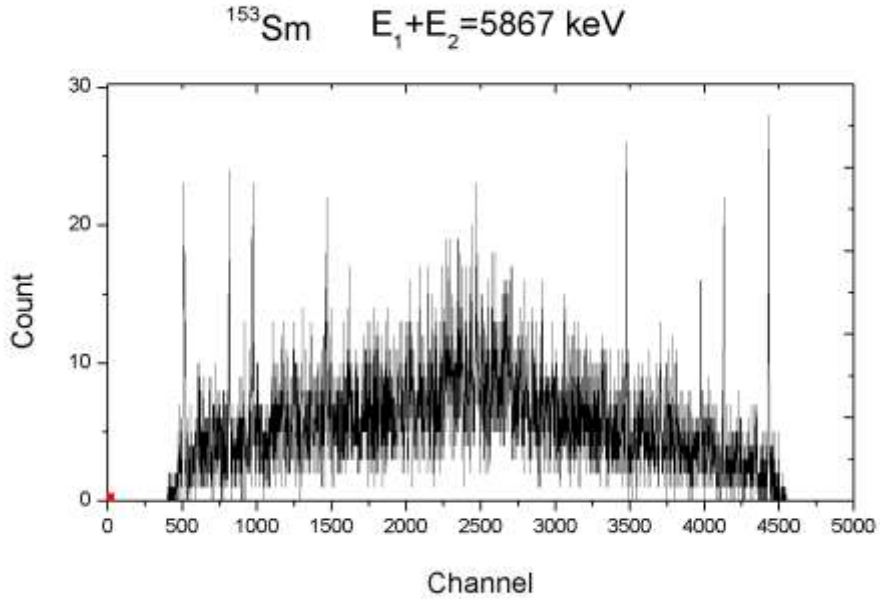

Fig. 3. Two-step cascade on ^{153}Sm ground states intensity distributions.

Data treatment processes was performed by programs developed by group of A.M. Sukhovoj at JINR.

Results and discussion

From 10 TCS spectrum correspond with ten detected peak in summation spectrum, transitions energy and intensities of 368 cascades were obtained. Absolute cascade intensities normalized to 10^6 decays are given in Table 1. Uncertainties of experimental cascade intensity were estimated to be few percent to approximately 50 percent, depending on intensity strength.

The distribution of $I_{\gamma\gamma} = F(E_1)$, which E_1 is primary gamma transition, was shown in Fig. 4. Intensities of cascade decay were calculated by comparing the relative intensity, which were directly obtained from TCS spectrum, with the strongest cascade transitions and their absolute values [8].

Experimental data were fitted with new model of approximation of $I_{\gamma\gamma}$ [4]. The dash line and full black circle in Fig 4 represents the best fit of 6 different variants of approximation. The agreement of the fit with experimental data contributes to confirm the conclusion in [4]. For most of stable nuclei-targets, it is possible to expect that new model [4] will describe measured data with the better accuracy than any existing models [9] can do it. The expected distribution of cascade intensities based on the statistical theory with model [10, 11] for ^{153}Sm is also shown in Fig. 4 for a comparison.

Fig. 4. Histogram is the sums of the experimental cascade intensities with their experimental errors in 0.5 MeV bins. Full point are the best fit for 6 different variants of approximation, triangle are the calculated spectra for model [10, 11] with k(M1)=const.

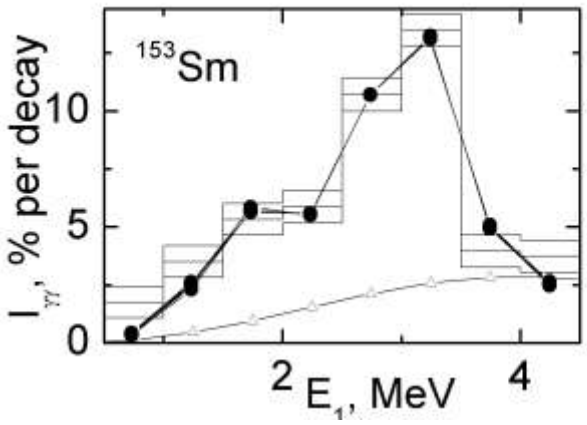

In Fig. 5, the level density was compared with model [10]. A mismatch in low energy region (< 3.5 MeV) between experimental values and models could be released. The strong deviation of observed radiative strength functions *k* with existing models [10,12,13] was shown in Fig. 6.

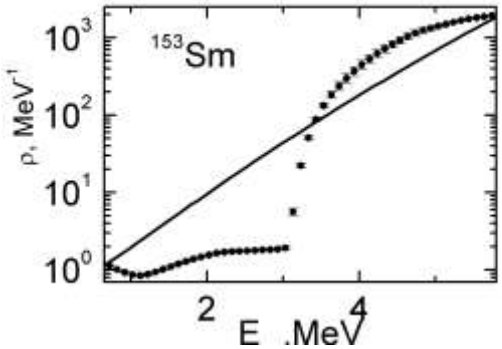

Fig. 5. The most probable mean densities of intermediate levels of two-step cascades (full point with the bars) and their variations in several (minimal number is 6) different variants of approximations with the lowest χ^2. Solid line is the data of [10].

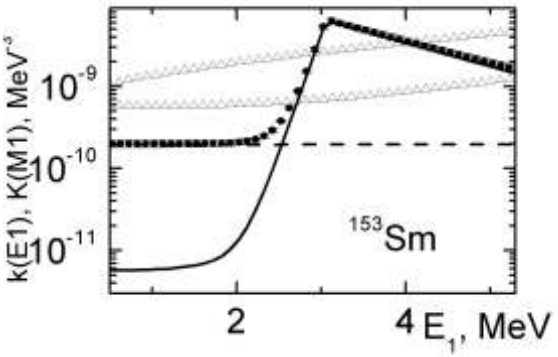

Fig. 6. The strength functions of E1-transitions (open points) and M1-transitions (dash lines). Solid line is their sums. Top triangles are the model calculation [13, 14], bottom triangles are the model calculation [11] in sum with k(M1)=const.

Conclusion

First, the results contributed to increase experimental data about the parameters of cascade gamma decay for compound states of even-odd nuclei.

Secondly, distribution of cascade intensities in function of primary gamma transition energy is accurately described by new model of calculation of nuclear properties in compound states [4].

Finally, the uncertainty of experimental data needs an improvement by increasing measurement time and using target with higher isotope abundance.

Table 1. Energies of primary E_1 and secondary E_2 transitions and their intermediate level E_i for nucleus ^{153}Sm. Values of the intensities, $i_{\gamma\gamma}$, are normalized to 10^6 decays.

E_1+E_2	E_1	E_i	E_2	$I_{\gamma\gamma}$		E_1+E_2	E_1	E_i	E_2	$I_{\gamma\gamma}$
5867.6	5242.4	625.2	625.2	2339		5685.1	5117.2	750.4	567.9	69
5867.6	5237.6	630.0	630.0	3801		5685.1	5021.2	846.4	663.9	75
5867.6	5130.1	737.5	737.5	533		5685.1	4777.9	1089.7	907.2	78
5867.6	5099.0	768.6	768.6	533		5685.1	4757.2	1110.4	927.9	66
5867.6	5080.6	787.0	787.0	602		5685.1	4695.7	1171.9	989.4	327
5867.6	4888.0	979.6	979.6	1892		5685.1	4584.6	1283.0	1100.5	156
5867.6	4883.3	984.3	984.3	2769		5685.1	4552.2	1315.4	1132.9	99
5867.6	4773.7	1093.9	1093.9	585		5685.1	4524.6	1343.0	1160.5	237
5867.6	4699.7	1168.0	1167.9	2546		5685.1	4512.7	1354.9	1172.4	213
5867.6	4665.2	1202.4	1202.4	464		5685.1	4464.5	1403.1	1220.6	75
5867.6	4508.3	1359.8	1359.3	413		5685.1	4200.6	1667.0	1484.5	114
5867.6	4501.3	1366.5	1366.3	636		5685.1	4127.8	1739.8	1557.3	315
5867.6	4477.8	1389.8	1389.8	808		5685.1	4063.9	1803.7	1621.2	114
5867.6	4464.5	1403.1	1403.1	361		5685.1	3982.1	1885.5	1703.0	129
5867.6	4456.2	1411.4	1411.4	757		5685.1	3935.3	1932.3	1749.8	201
5867.6	4448.6	1419.0	1419.0	1238		5685.1	3931.8	1935.8	1753.3	141
5867.6	4430.6	1437.0	1437.0	894		5685.1	3902.0	1965.6	1783.1	87
5867.6	4398.5	1469.1	1469.1	843		5685.1	3887.0	1980.6	1798.1	213
5867.6	4381.6	1486.0	1486.0	1703		5685.1	3821.7	2045.9	1863.4	177
5867.6	4355.0	1512.6	1512.6	1187		5685.1	3722.8	2144.8	1962.3	168
5867.6	4307.1	1560.5	1560.5	1101		5685.1	3709.8	2157.8	1975.3	222
5867.6	4281.2	1586.4	1586.4	447		5685.1	3694.1	2173.5	1991.0	108
5867.6	4263.6	1604.0	1604.0	705		5685.1	3677.6	2190.0	2007.5	216
5867.6	4241.9	1625.7	1625.7	1617		5685.1	3643.4	2224.2	2041.7	165
5867.6	4233.6	1634.0	1634.0	636		5685.1	3568.0	2299.6	2117.1	153
5867.6	4127.8	1739.8	1739.8	808		5685.1	3526.2	2341.4	2158.9	216
5867.6	4119.5	1748.1	1748.1	2219		5685.1	3500.2	2367.4	2184.9	153
5867.6	4115.0	1752.6	1752.6	2958		5685.1	3492.4	2375.2	2192.7	162
5867.6	4035.4	1832.3	1832.2	482		5685.1	3434.4	2433.2	2250.7	144
5867.6	4026.2	1841.4	1841.4	430		5685.1	3419.8	2447.8	2265.3	120
5867.6	3982.1	1885.5	1885.5	568		5685.1	3407.0	2460.6	2278.1	339
5867.6	3949.2	1918.4	1918.4	430		5685.1	3396.3	2471.3	2288.8	132
5867.6	3935.3	1932.3	1932.3	1617		5685.1	3388.1	2479.5	2297.0	207
5867.6	3731.6	2136.0	2136.0	430		5685.1	3375.0	2492.6	2310.1	288
5867.6	3694.1	2173.5	2173.5	894		5685.1	3358.5	2509.1	2326.6	168
5867.6	3628.1	2239.5	2239.5	808		5685.1	3324.9	2542.7	2360.2	165
5867.6	3620.1	2247.5	2247.5	860		5685.1	3320.0	2547.6	2365.1	168
5867.6	3557.7	2309.9	2309.9	860		5685.1	3250.0	2617.6	2435.1	129
5867.6	3452.9	2414.7	2414.7	1617		5685.1	3225.6	2642.0	2459.5	120

E_1+E_2	E_1	E_i	E_2	$I_{\gamma\gamma}$		E_1+E_2	E_1	E_i	E_2	$I_{\gamma\gamma}$
5867.6	3448.6	2419.0	2419.0	929		5685.1	3175.5	2692.1	2509.6	285
5867.6	3378.5	2489.1	2489.1	1101		5685.1	3168.9	2698.7	2516.2	351
5867.6	3372.1	2495.6	2495.5	1514		5685.1	3144.5	2723.1	2540.6	186
5867.6	3317.5	2550.1	2550.1	1617		5685.1	3065.5	2802.1	2619.6	120
5867.6	3285.1	2582.5	2582.5	843		5685.1	3012.5	2855.1	2672.6	195
5867.6	3260.7	2606.9	2606.9	722		5685.1	2987.9	2879.7	2697.2	291
5867.6	3195.7	2671.9	2671.9	980		5685.1	2980.6	2887.0	2704.5	156
5867.6	3175.5	2692.1	2692.1	1135		5685.1	2947.3	2920.3	2737.8	249
5867.6	3168.9	2698.7	2698.7	1273		5685.1	2927.5	2940.1	2757.6	237
5867.6	3147.7	2719.9	2719.9	1858		5685.1	2901.0	2966.6	2784.1	219
5867.6	3120.4	2747.2	2747.2	860		5685.1	2877.7	2989.9	2807.4	165
5867.6	3082.5	2785.1	2785.1	1410		5685.1	2862.7	3004.9	2822.4	237
5867.6	3068.2	2799.4	2799.4	1187		5685.1	2832.9	3034.7	2852.2	183
5867.6	3059.6	2808.1	2808.0	946		5685.1	2769.8	3097.8	2915.3	207
5867.6	3050.7	2816.9	2816.9	1135		5685.1	2761.5	3106.1	2923.6	267
5867.6	3021.2	2846.4	2846.4	1978		5685.1	2694.2	3173.4	2990.9	120
5867.6	2974.7	2892.9	2892.9	2098		5685.1	2659.8	3207.8	3025.3	138
5867.6	2441.4	3426.2	3426.2	550		5685.1	2486.4	3381.2	3198.7	174
5867.6	2390.7	3476.9	3476.9	636		5685.1	2390.7	3476.9	3294.4	114
5867.6	2333.7	3533.9	3533.9	1273		5685.1	2227.6	3640.0	3457.5	141
5867.6	2234.4	3633.2	3633.2	722		5685.1	2217.5	3650.1	3467.6	192
5867.6	2212.0	3655.6	3655.6	705		5685.1	2212.0	3655.6	3473.1	138
5867.6	2152.1	3715.5	3715.5	413		5685.1	2152.1	3715.5	3533.0	177
5832.8	5237.6	630.0	595.2	322		5591.9	5021.2	846.4	570.7	153
5832.8	5172.3	695.3	660.5	2597		5591.9	4966.4	901.2	625.5	264
5832.8	4950.8	916.8	882.0	756		5591.9	4933.4	934.2	658.5	279
5832.8	4695.7	1171.9	1137.1	826		5591.9	4883.3	984.3	708.6	414
5832.8	4665.2	1202.4	1167.6	357		5591.9	4862.8	1004.8	729.1	456
5832.8	4508.3	1359.8	1324.5	350		5591.9	4862.8	1004.8	729.1	462
5832.8	4477.8	1389.8	1355.0	385		5591.9	4665.2	1202.4	926.7	330
5832.8	4435.2	1432.4	1397.6	329		5591.9	4608.1	1259.5	983.8	351
5832.8	4419.0	1448.6	1413.8	490		5591.9	4584.6	1283.0	1007.3	342
5832.8	4341.1	1526.9	1491.7	630		5591.9	4562.3	1305.3	1029.6	354
5832.8	4313.0	1554.6	1519.8	420		5591.9	4552.2	1315.4	1039.7	282
5832.8	4200.6	1667.0	1632.2	532		5591.9	4540.2	1327.4	1051.7	399
5832.8	4133.2	1734.4	1699.6	665		5591.9	4524.6	1343.0	1067.3	366
5832.8	4098.9	1768.8	1733.9	476		5591.9	4477.8	1389.8	1114.1	534
5832.8	4082.6	1785.0	1750.2	322		5591.9	4464.5	1403.1	1127.4	657
5832.8	4077.5	1790.1	1755.3	658		5591.9	4456.2	1411.4	1135.7	411
5832.8	4035.4	1832.3	1797.4	560		5591.9	4430.6	1437.0	1161.3	372
5832.8	4026.2	1841.4	1806.6	931		5591.9	4410.1	1457.5	1181.8	585

E_1+E_2	E_1	E_i	E_2	$I_{\gamma\gamma}$		E_1+E_2	E_1	E_i	E_2	$I_{\gamma\gamma}$
5832.8	4019.0	1848.6	1813.8	630		5591.9	4398.5	1469.1	1193.4	720
5832.8	3968.9	1898.7	1863.9	714		5591.9	4393.0	1474.6	1198.9	612
5832.8	3935.3	1932.3	1897.5	1372		5591.9	4355.0	1512.6	1236.9	387
5832.8	3862.3	2005.3	1970.5	469		5591.9	4241.9	1625.7	1350.0	528
5832.8	3829.9	2037.7	2002.9	497		5591.9	4016.1	1851.5	1575.8	633
5832.8	3777.3	2090.6	2055.5	630		5591.9	3935.3	1932.3	1656.6	735
5832.8	3755.8	2111.8	2077.0	665		5591.9	3931.8	1935.8	1660.1	432
5832.8	3709.8	2157.8	2123.0	462		5591.9	3818.2	2049.4	1773.7	729
5832.8	3694.1	2173.5	2138.7	357		5591.9	3809.3	2058.3	1782.6	588
5832.8	3677.6	2190.0	2155.2	469		5591.9	3755.8	2111.8	1836.1	465
5832.8	3526.2	2341.4	2306.6	658		5591.9	3709.8	2157.8	1882.1	435
5832.8	3426.9	2440.7	2405.9	749		5591.9	3608.3	2259.3	1983.6	1236
5832.8	3375.0	2492.6	2457.8	707		5591.9	3573.4	2294.2	2018.5	663
5832.8	3277.4	2590.2	2555.4	343		5591.9	3557.7	2309.9	2034.2	420
5832.8	3270.6	2597.0	2562.2	966		5591.9	3522.1	2345.5	2069.8	636
5832.8	3250.0	2617.6	2582.8	693		5591.9	3448.6	2419.0	2143.3	474
5832.8	3195.7	2671.9	2637.1	903		5591.9	3419.8	2447.8	2172.1	708
5832.8	3187.4	2680.2	2645.4	1078		5591.9	3396.3	2471.3	2195.6	705
5832.8	3125.9	2741.7	2706.9	931		5591.9	3388.1	2479.5	2203.8	465
5832.8	3059.6	2808.1	2773.2	546		5591.9	3375.0	2492.6	2216.9	561
5832.8	3042.0	2825.6	2790.8	945		5591.9	3329.7	2537.9	2262.2	582
5832.8	3016.5	2851.1	2816.3	616		5591.9	3225.6	2642.0	2366.3	390
5832.8	3007.0	2860.6	2825.8	819		5591.9	3187.4	2680.2	2404.5	513
5832.8	2980.6	2887.0	2852.2	1197		5591.9	3077.0	2791.1	2514.9	720
5832.8	2974.7	2892.9	2858.1	1015		5591.9	3065.5	2802.1	2526.4	549
5832.8	2927.5	2940.1	2905.3	525		5591.9	3046.4	2821.4	2545.5	786
5832.8	2888.6	2979.0	2944.2	511		5591.9	2939.0	2928.6	2652.9	801
5832.8	2832.9	3034.7	2999.9	700		5591.9	2888.6	2979.0	2703.3	795
5832.8	2486.4	3381.2	3346.4	679		5591.9	2849.5	3018.1	2742.4	804
5832.8	2477.4	3390.2	3355.4	882		5591.9	2710.9	3156.7	2881.0	1059
5832.8	2333.7	3533.9	3499.1	546		5591.9	2694.2	3173.4	2897.7	591
5832.8	2217.5	3650.1	3615.3	630		5591.9	2486.4	3381.2	3105.5	384
5777.3	5117.2	750.4	660.1	656		5591.9	2477.4	3390.2	3114.5	540
5777.3	5047.0	820.6	730.3	288		5591.9	2441.4	3426.2	3150.5	525
5777.3	5039.7	827.9	737.6	266		5591.9	2390.7	3476.9	3201.2	729
5777.3	4987.3	880.3	790.0	256		5591.9	2212.0	3655.6	3379.9	660
5777.3	4757.2	1110.4	1020.1	272		5547.5	4697.6	1170.0	849.9	728
5777.3	4697.6	1170.0	1079.7	678		5547.5	4644.5	1223.1	903.0	498
5777.3	4508.3	1359.8	1269.0	310		5547.5	4545.3	1322.3	1002.2	367
5777.3	4456.2	1411.4	1321.1	435		5547.5	4469.6	1398.0	1077.9	367
5777.3	4355.0	1512.6	1422.3	685		5547.5	4456.2	1411.4	1091.3	122

E_1+E_2	E_1	E_i	E_2	$I_{\gamma\gamma}$		E_1+E_2	E_1	E_i	E_2	$I_{\gamma\gamma}$
5777.3	4330.0	1537.6	1447.3	573		5547.5	4381.6	1486.0	1165.9	498
5777.3	4298.7	1568.9	1478.6	448		5547.5	4330.0	1537.6	1217.5	103
5777.3	4254.1	1613.5	1523.2	384		5547.5	4310.6	1557.0	1236.9	945
5777.3	4091.8	1775.8	1685.5	368		5547.5	4063.9	1803.7	1483.6	475
5777.3	4077.5	1790.1	1699.8	230		5547.5	4026.2	1841.4	1521.3	456
5777.3	4072.4	1795.2	1704.9	352		5547.5	3995.4	1872.2	1552.1	249
5777.3	4026.2	1841.4	1751.1	765		5547.5	3935.3	1932.3	1612.2	489
5777.3	3995.4	1872.2	1781.9	723		5547.5	3448.6	2419.0	2098.9	597
5777.3	3862.3	2005.3	1915.0	413		5547.5	3372.1	2495.6	2175.4	728
5777.3	3829.9	2037.7	1947.4	442		5547.5	3175.5	2692.1	2372.0	714
5777.3	3755.8	2111.8	2021.5	525		5547.5	3125.9	2741.7	2421.6	996
5777.3	3688.2	2179.4	2089.1	470		5547.5	3036.4	2831.2	2511.1	738
5777.3	3602.9	2264.7	2174.4	486		5547.5	2939.0	2928.6	2608.5	794
5777.3	3573.4	2294.2	2203.9	720		5547.5	2888.6	2979.0	2658.9	869
5777.3	3522.1	2345.5	2255.2	707		5547.5	2832.9	3034.7	2714.6	766
5777.3	3444.3	2423.3	2333.0	416		5547.5	2694.2	3173.4	2853.3	743
5777.3	3372.1	2495.6	2405.2	685		5510.0	4777.9	1089.7	732.1	700
5777.3	3187.4	2680.2	2589.9	662		5510.0	4699.7	1168.0	810.3	2275
5777.3	3080.7	2786.9	2696.6	589		5510.0	4695.7	1171.9	814.3	700
5777.3	3046.4	2821.4	2730.9	579		5510.0	4508.3	1359.8	1001.7	705
5777.3	3016.5	2851.1	2760.8	598		5510.0	4355.0	1512.6	1155.0	1575
5777.3	2901.0	2966.6	2876.3	288		5510.0	4341.1	1526.9	1168.9	1030
5777.3	2888.6	2979.0	2888.7	483		5510.0	4263.6	1604.0	1246.4	800
5777.3	2769.8	3097.8	3007.5	934		5510.0	3829.9	2037.7	1680.1	530
5777.3	2635.5	3232.1	3141.8	406		5510.0	3821.7	2045.9	1688.3	675
5777.3	2333.7	3533.9	3443.6	570		5510.0	3784.3	2083.3	1725.7	800
5777.3	2234.4	3633.2	3542.9	621		5510.0	3777.3	2090.6	1732.7	905
5741.1	5172.3	695.3	568.8	281		5510.0	3743.0	2124.6	1767.0	900
5741.1	4777.9	1089.7	963.2	323		5510.0	3630.6	2237.0	1879.4	975
5741.1	4757.2	1110.4	983.9	334		5510.0	3620.1	2247.5	1889.9	920
5741.1	4697.6	1170.0	1043.5	809		5510.0	3557.7	2309.9	1952.3	1045
5741.1	4524.6	1343.0	1216.5	1767		5510.0	3077.0	2791.1	2433.0	1060
5741.1	4341.1	1526.9	1400.0	1170		5510.0	2974.7	2892.9	2535.3	925
5741.1	4214.5	1653.1	1526.6	578		5510.0	2939.0	2928.6	2571.0	870
5741.1	4127.8	1739.8	1613.3	471		5510.0	2710.9	3156.7	2799.1	1120
5741.1	4054.7	1812.9	1686.4	464		5510.0	2659.8	3207.8	2850.2	1425
5741.1	3982.1	1885.5	1759.0	513		5510.0	2635.5	3232.1	2874.5	1470
5741.1	3902.0	1965.6	1839.1	498		5510.0	2227.6	3640.0	3282.4	1050
5741.1	3829.9	2037.7	1911.2	399		5510.0	2152.1	3715.5	3357.9	1055
5741.1	3777.3	2090.6	1963.8	418		5489.0	4699.7	1168.0	789.3	756
5741.1	3667.1	2200.5	2074.0	608		5489.0	4693.5	1174.1	795.5	412

E_1+E_2	E_1	E_i	E_2	$I_{\gamma\gamma}$		E_1+E_2	E_1	E_i	E_2	$I_{\gamma\gamma}$
5741.1	3643.4	2224.2	2097.7	646		5489.0	4552.2	1315.4	936.8	1462
5741.1	3526.2	2341.4	2214.9	1208		5489.0	4549.1	1318.5	939.9	1243
5741.1	3419.8	2447.8	2321.3	817		5489.0	4512.7	1354.9	976.3	1739
5741.1	3375.0	2492.6	2366.1	551		5489.0	4508.3	1359.8	980.7	790
5741.1	3329.7	2537.9	2411.4	452		5489.0	4501.3	1366.5	987.7	748
5741.1	3250.0	2617.6	2491.1	669		5489.0	4346.5	1521.1	1142.5	731
5741.1	3225.6	2642.0	2515.5	661		5489.0	4341.1	1526.9	1147.9	756
5741.1	3175.5	2692.1	2565.6	429		5489.0	4098.9	1768.8	1390.1	823
5741.1	3168.9	2698.7	2572.2	958		5489.0	4035.4	1832.3	1453.6	865
5741.1	3155.2	2712.4	2585.9	851		5489.0	3777.3	2090.6	1711.7	874
5741.1	3120.4	2747.2	2620.7	486		5489.0	3454.0	2413.6	2035.0	504
5741.1	3016.5	2851.1	2724.6	760		5489.0	3371.7	2495.9	2117.3	529
5741.1	2947.3	2920.3	2793.8	714		5489.0	3277.4	2590.2	2211.6	605
5741.1	2939.0	2928.6	2802.1	771		5489.0	3228.6	2639.0	2260.4	874
5741.1	2911.2	2956.4	2829.9	574		5489.0	3153.6	2714.0	2335.4	932
5741.1	2895.3	2972.3	2845.8	578		5489.0	3059.6	2808.1	2429.4	874
5741.1	2888.6	2979.0	2852.5	851		5489.0	3046.4	2821.4	2442.6	840
5741.1	2769.8	3097.8	2971.3	783		5489.0	2932.7	2934.9	2556.3	840
5741.1	2761.5	3106.1	2979.6	319		5489.0	2895.3	2972.3	2593.7	781
5741.1	2659.8	3207.8	3081.3	635		5489.0	2885.4	2982.2	2603.6	386
5741.1	2441.4	3426.2	3299.7	391		5489.0	2802.5	3065.1	2686.5	840
5741.1	2333.7	3533.9	3407.4	1015						
5741.1	2234.4	3633.2	3506.7	745						

References

[1] S.T. Boneva, V.A. Khitrov, A.M. Sjkhovoj, Nucl. Phys. A **589** (1995) 293.
[2] Vasilieva E.V., Sukhovoj A.M., Khitrov V.A., Phys. At. Nucl., **64**(2) (2001) 153. P. 15.
[3] Sukhovoj A.M., Khitrov V.A., Phys. Part. Nucl., **36** (2005) 359.
[4] A.M. Sukhovoj, L.V. Mitsyna, in: *Proceedings of XXII International Seminar on Interaction of Neutrons with Nuclei, Dubna, May 2014*, Preprint № E3-2015-13, (Dubna, 2015) p.245.
[5] A.M. Sukhovoj, V.A. Khitrov. Sov. J. Prib. Tekhn. Eksp. **5** (1984) 27.
[6] A.M. Sukhovoj, V.A. Khitrov, Instr. Exp. Tech. **27** (1984) 1071
[7] S.T. Boneva, V.A. Khitrov, Yu.V. Kholnov, V.D. Kulik, Le Hong Khiem, Pham Dinh Khang, Yu.P. Popov, A.M. Sukhovoj, E.V. Vasilieva : On the construction of a complex gamma decay scheme on the basis of the spectroscopic data from (n,2γ) and (n, γ) - American Institute of Physics Conference Proceedings, Vol.**238** (1990), p.485-487 (ISBN 978-0-7354-0537-0, ISSN 0094-243X).
[8] http://www.bnl.gov/ENSDF
[9] Reference Input Parameter Library 2002. Handbook for calculations of nuclear reaction data (IAEA-TECDOC, 2002).
[10] Kadmenskij S.G., Markushev V.P., Furman W.I., Sov. J. Nucl. Phys., **37** (1983) 165.
[11] Dilg W., Schantl W., Vonach H., Uhl M., Nucl. Phys., **217**(1973) 269.
[12] Научно-Технический Центр "Стабильные Изотопы", Сертификат Качества №343.
[13] Axel P., Phys. Rev., **126**, (1962) 671.
[14] Brink D.M., Ph.D. Thesis. Oxford University, 1955.